Journal of Medical Devices Technology
jmeditec.utm.my

Original Research

Fabrication and Characterization of a PEGDMA-Conjugated Patch for Epicardial Cardiac Applications

Rishatani Gunasegaran[1,2], Rania Hussien Al-Ashwal[1,2*], Norhana Jusoh[2], Muhammad Hanif bin Ramlee[2], Sadeq M. Al-Hazmy[3]

[1]Advanced Diagnostic and Progressive Human Care Research group, Health and Wellness Research Alliance, Universiti Teknologi Malaysia, 81310, Johor Bahru, Johor, Malaysia
[2]Department of Biomedical Engineering and Health Sciences, Faculty of Electrical Engineering, Universiti Teknologi Malaysia, Johor Bahru 81310, Johor, Malaysia
[3]Department of Chemistry, College of Science, Qassim University, Buraidah 51452, Saudi Arabia

ARTICLE INFO

Article History:
Received 18 June 2025
Accepted 1 August 2025
Available online 2 August 2025

Keywords:
Conductivity,
Epicardium,
Nanostructures,
Hydrogel,
Myocardium

ABSTRACT

This study aims to fabricate and characterize a conductive cardiac patch incorporating green-synthesized silver nanoparticles (Api-AgNPs) tailored for epicardial applications. The biosynthesis yielded uniformly dispersed nanostructures with favorable stability and functional surface chemistry. Characterization techniques, including Field Emission Scanning Electron Microscopy (FESEM), Dynamic Light Scattering (DLS), Fourier Transform Infrared Spectroscopy (FTIR), and zeta potential measurements, were used to confirm size distribution, surface functionality, and colloidal stability. FESEM analysis revealed predominantly spherical nanoparticles with an average size of 98.84 ± 43.98 nm based on manual measurements, while automated ImageJ analysis yielded a mean of 13.86 ± 9.13 nm after outlier correction. Upon incorporation into a PEGDMA hydrogel matrix, the particles maintained uniform dispersion and reduced apparent size (42–80 nm), indicating effective spatial separation. DLS analysis showed a hydrodynamic diameter of 113.73 ± 1.17 nm with a polydispersity index (PDI) of 0.40 ± 0.005, reflecting acceptable size uniformity. FTIR spectra confirmed key functional groups, hydroxyl (O–H), carbonyl (C=O), and aromatic (C–C), involved in nanoparticle stabilization and conductivity. A zeta potential of 40.9 ± 1.17 mV indicated strong colloidal stability. Electrical functionality was demonstrated by embedding the nanomaterial in a closed circuit, which successfully powered an LED. These findings underscore the potential of the Api-AgNP-integrated hydrogel as a conductive and biocompatible component in epicardial patches for myocardial repair, supporting the advancement of multifunctional cardiac tissue engineering strategies.

INTRODUCTION

Cardiovascular diseases (CVDs) are the leading cause of mortality worldwide, accounting for approximately 17.9 million deaths annually. Among these, myocardial infarction (MI) is a predominant condition, characterized by necrosis of cardiomyocytes due to restricted blood flow to the heart muscle (Tsao et al., 2022; Zheng et al.., 2021). Myocardial infarction leads to irreversible loss of cardiomyocytes and fibrotic remodeling of the myocardium, disrupting both the mechanical and electrical integrity of the heart. The resulting fibrotic scar is stiff, non-contractile, and electrically resistive, impeding synchronized contraction and worsening cardiac dysfunction (Hinderer & Schenke-Layland, 2019; Wei et al., 2023).

To address these complications, cardiac patches have been developed to provide mechanical support and aid in functional recovery. Recent innovations emphasize not only structural

*Rania Hussien Al-Ashwal (rania@utm.my)

Advanced Diagnostic and Progressive Human Care research group, Health and Wellness Research Alliance, Universiti Teknologi Malaysia, 81310, Johor Bahru, Johor, Malaysia

© 2025 Penerbit UTM Press. All rights reserved

reinforcement, such as auxetic designs for mechanical mimicry, but also restoration of electrical conduction across infarcted areas, which is critical for synchronized myocardial activity (Wei et al., 2023; Song et al., 2021). To promote electrical conductivity, materials such as carbon nanotubes, polypyrrole, MXenes, and gold or silver nanoparticles have been integrated into hydrogel matrices. These conductive materials facilitate the propagation of action potentials and help maintain continuous electrical signaling, thereby reducing the risk of arrhythmias and heart failure.

Silver (Ag) is one of the most promising conductive materials for tissue engineering, owing to its high electrical conductivity (~5.8 × 10^5 S/cm) and inherent antibacterial properties (Agarwala, 2020; Liang et al., 2023; Nguyen et al., 2016). However, bulk silver and unmodified silver nanoparticles (AgNPs) are associated with cytotoxicity, oxidative stress, and pro-inflammatory responses that can impair tissue regeneration and limit their biomedical utility (Shao et al., 2023). While electrical conductivity is vital, ensuring biocompatibility is equally essential to prevent adverse biological effects following implantation.

To overcome these limitations, green-synthesized AgNPs have emerged as a safer alternative. These biosynthesized nanoparticles are generally smaller, more stable, and less cytotoxic, with improved clearance from the body (Talarska et al., 2021; Haripriyaa et al., 2023; Hasan et al., 2018). AgNPs have demonstrated utility in wound healing, biosensing, vascular grafts, and drug delivery (Xu et al., 2020; Ghiuță & Cristea, 2020; Younis et al., 2021). In cardiovascular applications, they have been used in cardiac stents and scaffolds to improve conductivity and reduce infection risk (Hosoyama, 2017; Sheikh & Shahrajabian 2021; Alkhalaf et al., 2020). Nonetheless, risks such as oxidative stress and cardiotoxicity remain if parameters such as particle size, surface charge, and capping agent are not well-controlled (Olugbodi et al., 2023; Li et al., 2021; El-Baz et al., 2023).

Controlling nanoparticle size and shape is therefore critical for cardiovascular applications. Nanoparticles below 150 nm are considered optimal for cellular uptake and clearance (Al-Ansari et al., 2020; Abdel-Aty et al., 2023; Mohammed et al., 2018). Moreover, the biological behavior of AgNPs, whether antioxidant or pro-oxidant, is strongly influenced by the choice of reducing and stabilizing agents during synthesis (Hosoyama, 2017; Alkhalaf et al., 2020).

Green synthesis offers a biocompatible and environmentally friendly method for producing AgNPs, utilizing plant-derived or microbial agents to reduce silver ions and stabilize the nanoparticles. Among plant-based compounds, apigenin, a flavonoid found in various medicinal herbs, stands out due to its antioxidant, anti-inflammatory, and cardioprotective properties (Thomas et al., 2023; Raberi et al., 2022; Hemlata et al., 2020). Apigenin has previously been used in the green synthesis of gold nanoparticles with enhanced biocompatibility and therapeutic potential Mukaratirwa-Muchanyereyi et al., 2022; Liang et al 2019).

This study aims to biosynthesize silver nanoparticles using apigenin and evaluate their physicochemical characteristics, particularly size and morphology, for potential cardiac patch applications. Furthermore, these apigenin-capped AgNPs are embedded into a PEGDMA-based hydrogel matrix to assess their ability to enhance electrical conductivity and structural integration for epicardial patch use.

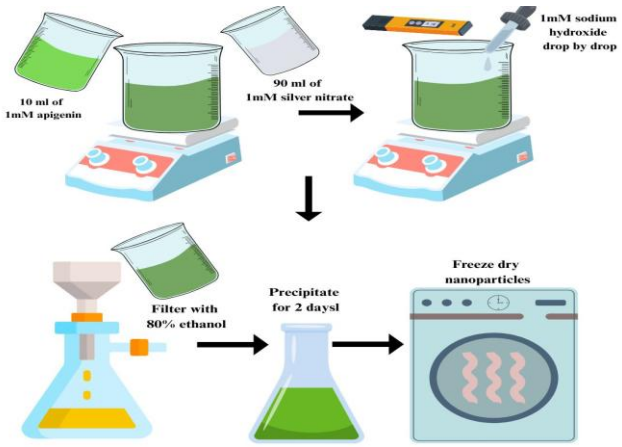

Fig.1 Flow diagram of biosynthesis of silver nanoparticles

MATERIALS AND METHOD

Freeze drying of the synthesized nanoparticles

After the sedimentation of the nanoparticles observed, the solution was separated centrifuged at 10000 rpm for 20 min and repeated for three times. Then, the solution was decanted using distilled water and freeze dried at -40 °C overnight. The freeze dried nanoparticles (Api-AgNPs) was stored at 4 °C (Sarangi et al., 2017). A green synthesis approach was adopted to produce a conductive nanocomponent for integration into an epicardial cardiac patch. The process began with the biosynthesis of apigenin-mediated silver nanoparticles (Api-AgNPs), followed by freeze-drying to yield a stable nanopowder suitable for further characterization. To synthesize the nanoparticles, 1 mM apigenin solution was prepared by dissolving apigenin in deionized water. Subsequently, 10 mL of the apigenin solution was added to 90 mL of 1 mM aqueous silver nitrate solution. The reaction mixture was heated at 40 °C with constant stirring, and sodium hydroxide (1 mM) was added gradually until the solution reached a basic pH of 10. To prevent photoactivation of silver ions, the container was wrapped in aluminum foil. After complete reaction, the solution was filtered dropwise into 80% ethanol. The mixture was then refrigerated at 4 °C for 72 hours to allow nanoparticle precipitation, as illustrated in Fig. 1.

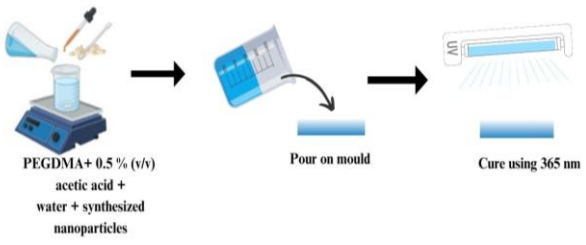

Fig.2 Synthesis of PEGDMA hydrogel

© 2025 Penerbit UTM Press. All rights reserved

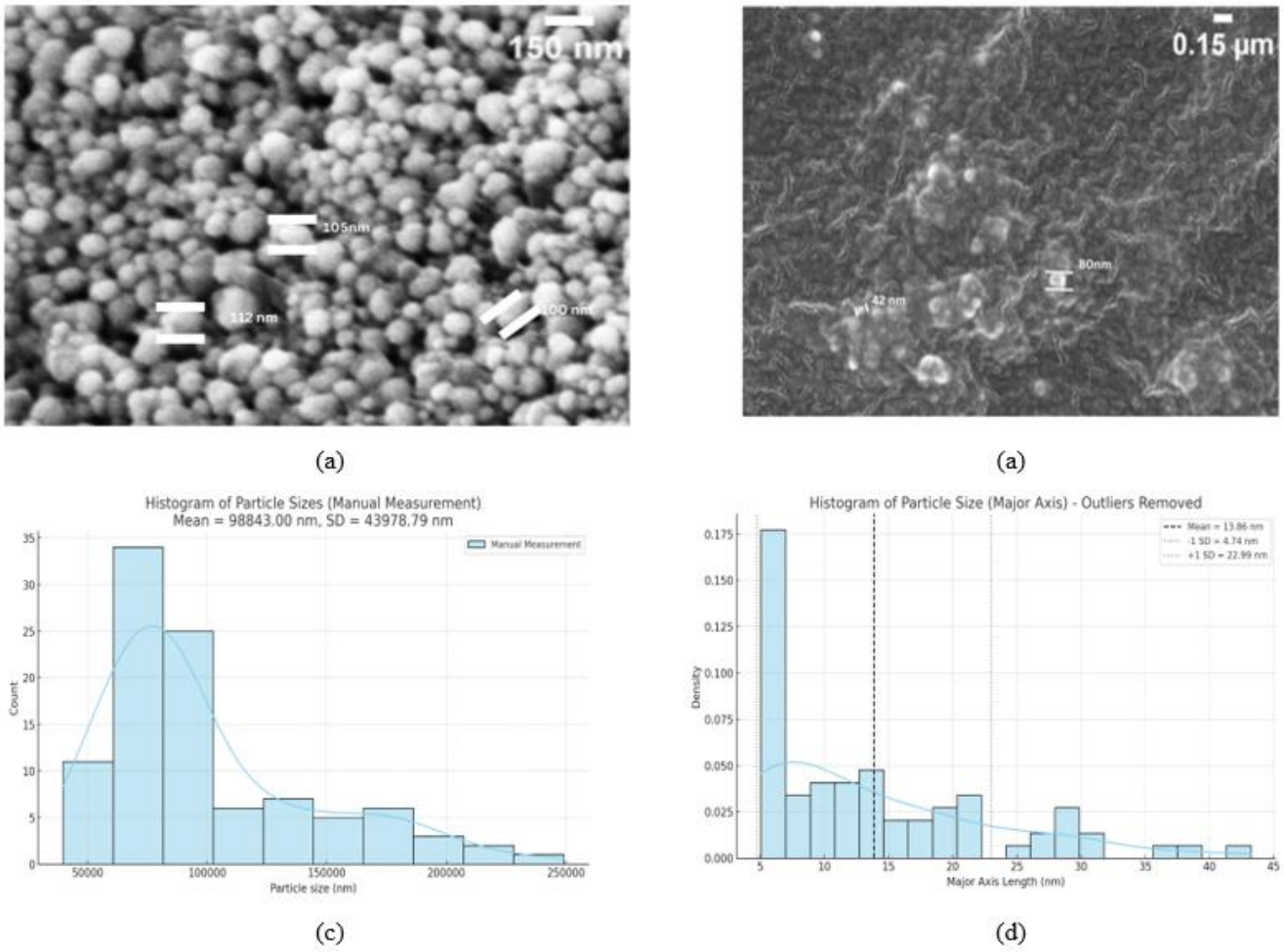

Fig.3 Field Emission Scanning Electron Microscopy (FESEM) images and particle size analysis of apigenin-mediated silver nanoparticles (Api-AgNPs). (a) FESEM micrograph of Api-AgNPs before hydrogel embedding, showing spherical morphology and relatively uniform distribution. (b) FESEM micrograph of Api-AgNPs embedded within PEGDMA hydrogel matrix, indicating improved separation and smaller apparent size. Histograms of silver nanoparticle size distribution. (c) Manual ImageJ measurement of 100 outlined particles, showing a mean size of 98.8 nm (SD ±44.0 nm). (d) Automated ImageJ analysis of 86 particles (outliers excluded), with a mean size of 13.9 nm (SD ±9.1 nm). Each graph includes normal distribution curves and standard deviation bands.

For hydrogel matrix fabrication, a photo crosslinking technique was employed. A polymeric precursor consisting of poly (ethylene glycol) (PEG, Mw = 4000), methacrylic anhydride and 2-hydroxy-2-methylpropiophenone (photoinitiator) was dissolved in 0.5% (v/v) acetic acid and stirred at 50 °C. The freeze-dried Api-AgNPs (1 mg) were incorporated into the solution, followed by thorough mixing to ensure uniform dispersion. The resulting formulation was cast into a mold and exposed to UV light (365 nm) for 30 minutes to induce photo-crosslinking, yielding a soft, elastic hydrogel that mimics the mechanical properties of myocardial tissue.

Fabrication of PEGDMA hydrogel matrix

Initially, the PEGDMA polymer was synthesized via a chemical modification method utilizing microwave scintillation, following established protocols (Njud et al., 2022; Song et al., 2021). For hydrogel preparation, the polymer was dissolved in 0.5% (v/v) acetic acid solution at 50 °C. The biosynthesized nanoparticles were then added to the polymer solution and mixed continuously to ensure uniform dispersion. Subsequently, 0.05% (w/v) of 2-hydroxy-2-methylpropiophenone was introduced as a photoinitiator, and the mixture was stirred thoroughly. A total of 1 mg of freeze-dried apigenin-mediated silver nanoparticles was incorporated into the formulation. After complete mixing, the solution was cast into a mold and subjected to photo-crosslinking via UV irradiation at 365 nm for 30 minutes, as illustrated in Fig. 2 (Song et al., 2021; Mekonnen et al., 2017).

Characterizations

a) Morphological Characterization

The morphology and particle dispersion of the biosynthesized apigenin-mediated silver nanoparticles (Api-AgNPs) were examined using Field Emission Scanning Electron Microscopy (FESEM) at 10,000× magnification and an accelerating voltage of 10 kV. Analyses were conducted on both free-standing nanoparticles and those incorporated into PEGDMA hydrogels.

© 2025 Penerbit UTM Press. All rights reserved

Samples were dried and sputter-coated with a ~5 nm gold layer to enhance conductivity prior to imaging. Images were captured using a secondary electron (SE) detector. Quantitative particle size analysis was performed using ImageJ software (NIH, USA), calibrated against a 150 nm embedded scale bar. Two independent approaches were used: Manual Measurement: A total of 100 well-defined, non-overlapping particles were manually selected and outlined using the polygon selection tool. The maximum diameter was recorded for each particle. Automated Measurement: Binarized FESEM images were analyzed using ImageJ's thresholding and particle analysis tools. The "Major Axis" parameter was extracted as an estimate of particle size. To ensure statistical robustness, outliers below 5 nm and above 200 nm were excluded. Histograms with kernel density estimation (KDE) curves and ±1 standard deviation (SD) markers were generated to compare size distribution across both methods.

b) Chemical Characterization

Fourier Transform Infrared Spectroscopy (FTIR) was employed to identify functional groups and confirm the capping and reducing role of apigenin in nanoparticle synthesis. FTIR spectra were recorded for powdered apigenin and freeze-dried Api-AgNPs using a [insert FTIR model, if available], with scans performed in triplicate over the wavenumber range of 4000–650 cm^{-1}.

c) Optical Characterization

Optical properties of the synthesized nanoparticles were assessed using a UV–Visible spectrophotometer. Triplicate measurements were performed to monitor the reduction of silver nitrate and confirm nanoparticle formation. Absorbance spectra were recorded in the range of 220–700 nm with a 1 nm resolution.

d) Particle Size and Zeta Potential

Dynamic Light Scattering (DLS) analysis was carried out using a Nano-ZS particle size analyzer (Malvern Instruments Ltd., UK) to determine the average particle diameter, polydispersity index (PDI), and zeta potential of the Api-AgNPs. Measurements were conducted in triplicate, with deionized water as the dispersant. Polystyrene latex (RI = 1.590, absorption = 0.010) was used as the reference standard.

e) Electrical Conductivity

To assess electrical conductivity, the hydrogel patches—with and without embedded Api-AgNPs—were integrated into a simple closed-loop circuit. An LED indicator was used to demonstrate current flow through the hydrogel matrix, confirming the conductive behavior conferred by nanoparticle incorporation.

RESULT AND DISCUSSION

Formation of biosynthesized apigenin mediated- silver nanoparticles

The morphology and size distribution of apigenin-mediated silver nanoparticles (Api-AgNPs) were evaluated using Field Emission Scanning Electron Microscopy (FESEM) at 10,000× magnification and an accelerating voltage of 10 kV. Prior to imaging, the samples were gold-sputtered (~5 nm) to enhance conductivity. ImageJ software, calibrated to a 150 nm scale bar,

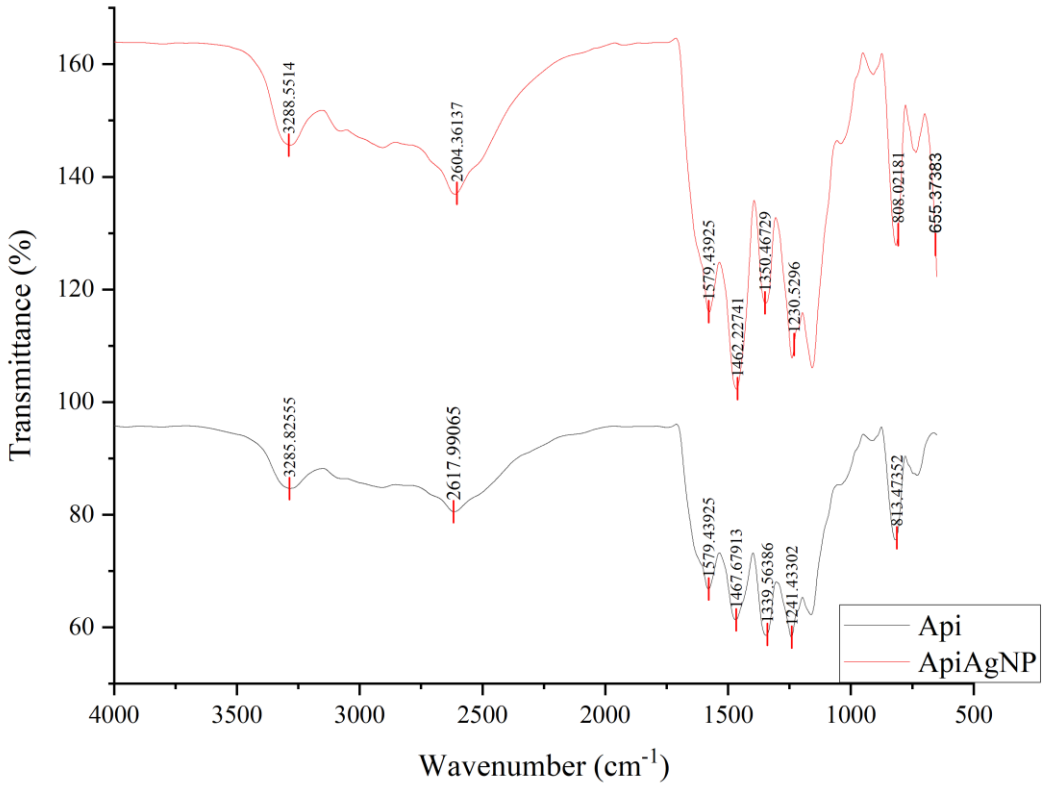

Fig.4. FTIR spectra for apigenin (black) and apigenin conjugated silver nanoparticles (red)

© 2025 Penerbit UTM Press. All rights reserved

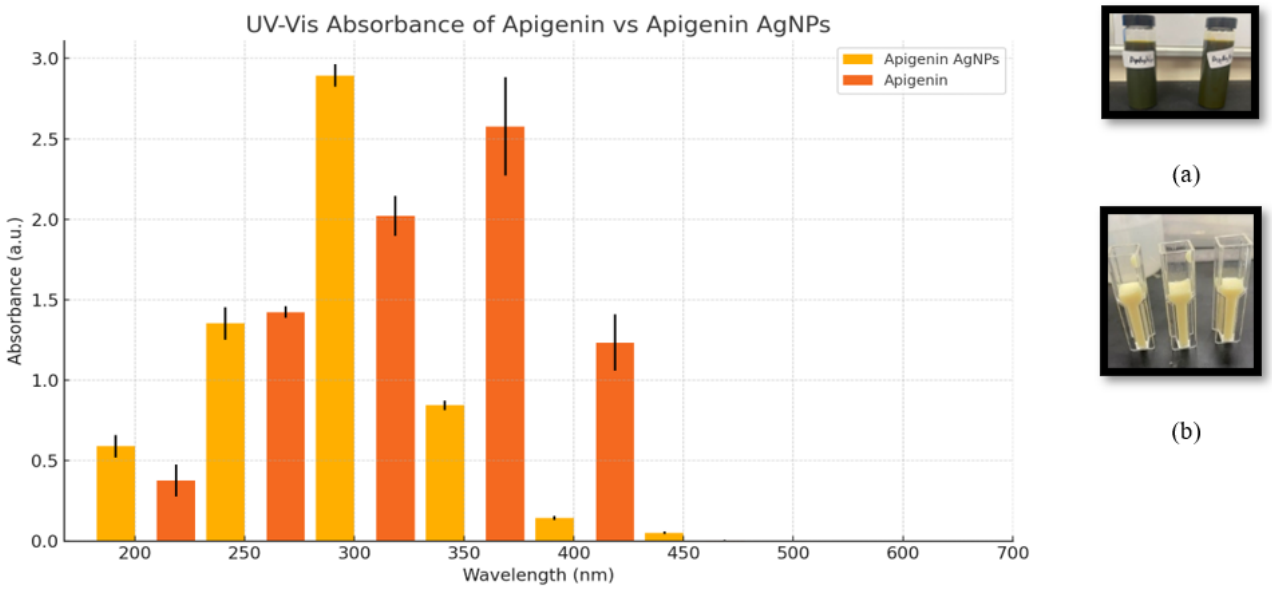

Fig. 5 UV–Vis absorbance spectra of Apigenin and Apigenin–silver nanoparticles (AgNPs) at selected wavelengths (200–700 nm). Bars represent the mean absorbance values from triplicate measurements for each sample. Error bars indicate the standard deviation (±SD). Samples used for measurments (a) Apigenin (b) Apigenin mediated Silver Nanoparticles

was employed for both manual and automated particle size analysis (Sarangi et al., 2017). The corresponding micrographs and histograms are presented in Fig. 3.

As shown in Fig. 3a, the unembedded Api-AgNPs exhibited predominantly spherical morphology and a relatively uniform dispersion. Manual analysis of 100 non-overlapping particles (Fig. 3c) revealed an average particle size of 98.84 ± 43.98 nm, with most particles distributed between 60 and 140 nm. This moderate size variability is characteristic of biosynthetic nanoparticle formation (Talabani et al., 2021).

Automated analysis, performed using ImageJ's thresholding and particle analyzer tools, assessed 86 particles and yielded a lower mean size of 13.86 ± 9.13 nm (Fig. 3d), reflecting the detection of smaller or fragmented particles. Outliers above 200 nm were excluded to normalize the distribution.

The discrepancy between the two measurement approaches is attributed to methodological differences: manual analysis focuses on well-defined, intact particles, while automated analysis captures a broader particle population, including clusters and low-contrast features (Cervantes et al., 2019). Nonetheless, both methods confirmed the spherical morphology and nanoscale dimensions (<150 nm) of the synthesized Api-AgNPs.

Following integration into the PEGDMA hydrogel, the Api-AgNPs retained their spherical shape and displayed enhanced spatial separation (Fig. 3b). Manual measurements post-embedding showed a reduced size range (42–80 nm), suggesting improved stabilization by the hydrogel matrix (Mohammed et al., 2018).

These findings collectively confirm that the PEGDMA hydrogel preserves nanoparticle morphology, prevents agglomeration, and maintains sub-150 nm dimensions. Such characteristics are crucial for biomedical applications, particularly in cardiac patches, where uniform nanoscale dispersion ensures mechanical compatibility and biofunctional performance (Mariadoss et al., 2019).

FTIR Characterization of Apigenin and Api-AgNPs

FTIR spectroscopy (Perkin Elmer) was employed to identify the functional groups involved in the reduction and stabilization of the synthesized nanoparticles. The FTIR spectrum of pure apigenin exhibited major absorption bands at 3285.83, 2617.99, 1579.44, 1462.22, 1339.56, 1241.43, 813.47, and 655.37 cm^{-1} (Fig. 4, red), corresponding to O–H stretching, C–H bending, C=O stretching, and C–C stretching. These findings are consistent with literature reports on the characteristic peaks of apigenin.

In comparison, the spectrum of the synthesized Api-AgNPs displayed peaks at 3288.55, 2604.36, 1579.44, 1462.22, 1350.46, and 808.20 cm^{-1} (Fig. 4, black), indicating that the key functional groups from apigenin were preserved and involved in the nanoparticle formation. The observed shifts in peak positions suggest successful reduction and capping, likely mediated by the hydroxyl and carboxyl groups of apigenin.Additionally, the peak at 655.37 cm^{-1} confirms the presence of silver, reflecting the metallic nature of the nanoparticles. These results support the role of apigenin as both a reducing and stabilizing agent in the green synthesis process. The retention of bioactive apigenin within the nanoparticle matrix further suggests potential cardio-protective functionality when applied as part of a conductive cardiac patch.

© 2025 Penerbit UTM Press. All rights reserved

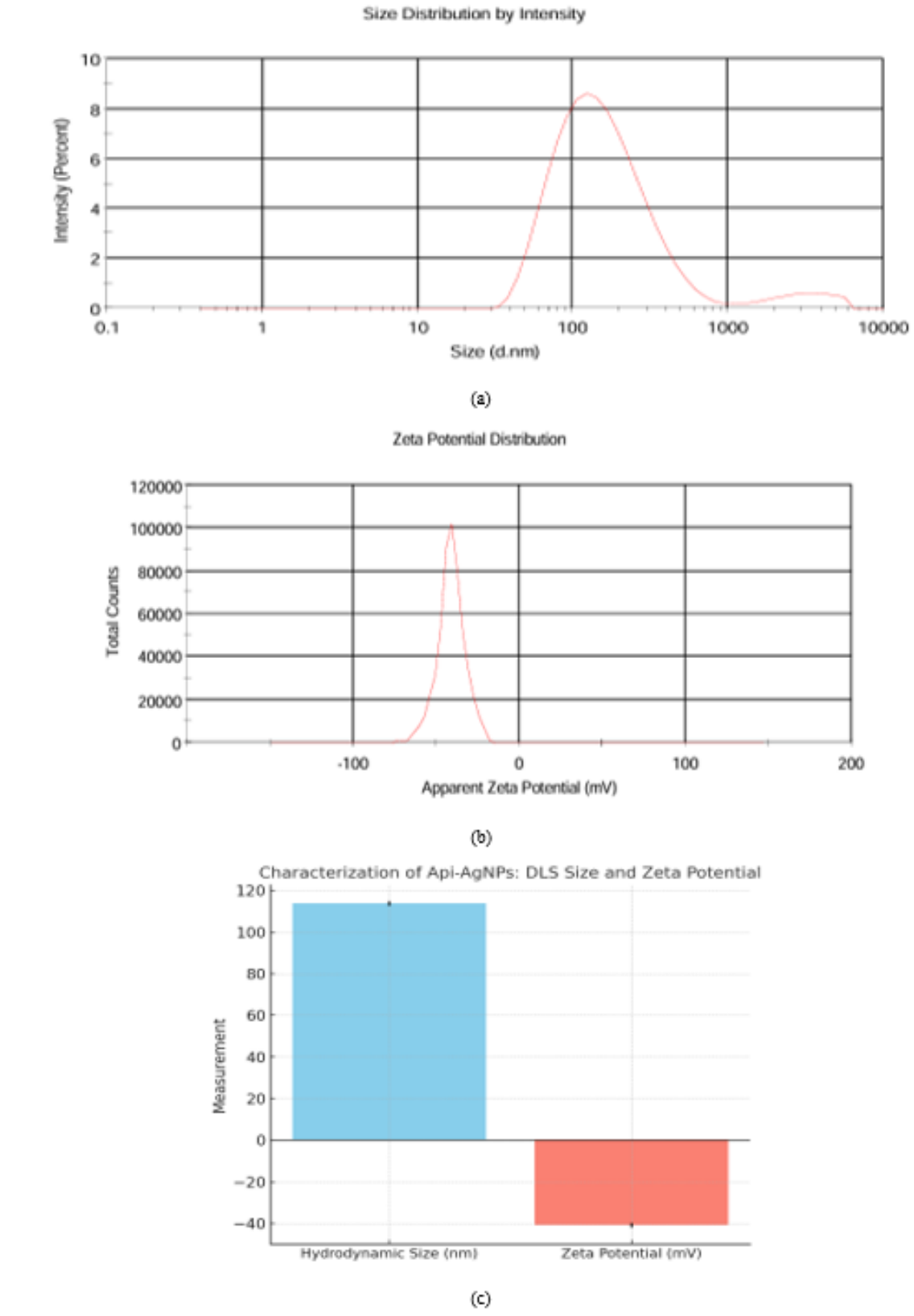

Fig.6 Nanoparticle size measurements: (a) size and PDI analysis; (b) ζ-potential of the biosynthesized Api-AgNPs. (c) DLS size and zeta potential of the Api-AgNPs with their respective standard deviations. Data are presented as mean ± standard deviation (n = 3).

© 2025 Penerbit UTM Press. All rights reserved

UV–Visible Spectroscopy Confirming Nanoparticle Formation

The UV–Vis absorption spectra of apigenin and the biosynthesized apigenin–silver nanoparticles (AgNPs) are shown in Figure 5. The apigenin solution exhibited a distinct absorbance peak at 350 nm, which aligns with previously reported findings, confirming the presence of its characteristic flavone chromophore (Swati Jaast & Anita Grewal 2021; Shakeel Ahmed et al., 2016). Some studies have also reported dual peaks near 260 nm and 350 nm, attributed to variations in plant source and extraction method (Ekren et al., 2007). In contrast, the biosynthesized AgNPs showed a broad absorption peak centered around 400 nm, corresponding to the surface plasmon resonance (SPR) phenomenon commonly observed in metallic nanoparticles (Shakeel Ahmed et al., 2016). This red shift and band broadening from 350 nm to 400 nm indicate the successful formation of AgNPs through the reduction of silver ions by apigenin. The SPR peak is attributed to the collective oscillation of conduction electrons on the nanoparticle surface, influenced by particle size, shape, interparticle spacing, and dielectric environment (Ekren et al., 2007; Shakeel Ahmed et al., 2016).

These findings are consistent with earlier green synthesis studies, where SPR peaks have been reported in the 400–420 nm range, depending on the synthesis method and nature of the plant-based reducing agent (Wan Mat Khalir et al., 2020; Shakeel Ahmed et al., 2016). Therefore, UV–Vis spectroscopy confirms the structural integrity of apigenin and the successful biosynthesis of AgNPs, validating apigenin's dual role as a reducing and stabilizing agent.

Particle Stability and Dispersion Analysis via DLS and Zeta Potential

The hydrodynamic diameter, polydispersity index (PDI), and zeta potential (ζ-potential) of the biosynthesized conductive nanomaterial were evaluated using dynamic light scattering (DLS) and electrophoretic light scattering. Prior to analysis, nanoparticle suspensions were diluted with deionized water to reduce multiple scattering effects.

As shown in Fig. 6, the Api-AgNPs exhibited a hydrodynamic diameter of 113.73 ± 1.17 nm, a PDI of 0.40 ± 0.005, and a zeta potential of -40.9 ± 1.17 mV, indicating moderate size uniformity and excellent colloidal stability. The hydrodynamic size is typically larger than the dry-state dimensions observed via FESEM, due to the inclusion of the solvation shell and potential weak aggregation.

Nanoparticles with diameters below 150 nm and PDI values between 0.3 and 0.5 are considered appropriate for biomedical applications and endocytosis pathways (Alexis et al., 2008; (Danaei et al., 2018). The observed values align with previous reports on biosynthesized AgNPs using plant extracts, such as red apple fruit. The strong negative zeta potential indicates significant electrostatic repulsion between particles, promoting dispersion stability and preventing agglomeration during formulation (Danaei et al., 2018).

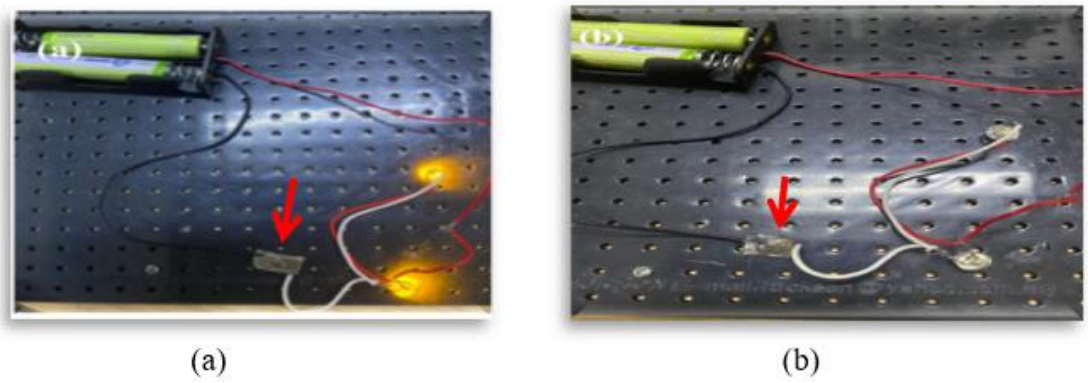

Fig.7 Electrical conductivity demonstration using a closed circuit system. Red arrow indicate the hydrogel. (a) Hydrogel embedded with biosynthesized Api-AgNPs completing the circuit and successfully illuminating the LED, indicating effective electron transfer through the composite. (b) Control hydrogel without nanoparticles, failing to complete the circuit, demonstrating lack of conductivity.

Conductivity Evaluation of Synthesized Composite

To assess the electrical conductivity of the biosynthesized nanocomposite, PEGDMA hydrogel patches with and without Api-AgNPs were incorporated into a simple closed circuit. Two light-emitting diodes (LEDs) were positioned across each patch to evaluate current transmission. As shown in Fig. 7(a), the LED illuminated when the nanoparticle-loaded hydrogel was inserted, indicating successful electron flow through the composite. Conversely, the control patch lacking Api-AgNPs failed to complete the circuit, and the LED remained unlit (Fig. 7(b)). These findings confirm that the biosynthesized nanomaterial retained its conductive properties within the hydrogel matrix.

CONCLUSION

The apigenin-mediated silver nanoparticles exhibited an average size of 98.84 ± 43.98 nm as observed in FESEM analysis (manual measurement), confirming their potential suitability for cardiovascular applications. The hydrodynamic diameter, measured using dynamic light scattering (DLS), was 113.73 ± 1.17 nm, which falls below the 150 nm threshold considered favorable for cellular uptake. FTIR spectroscopy

© 2025 Penerbit UTM Press. All rights reserved

confirmed the presence of functional groups from apigenin, including hydroxyl (O–H), carbonyl (C=O), and aromatic (C–C) bonds, which contribute to nanoparticle stabilization.

The polydispersity index (PDI) was 0.40 ± 0.005, indicating a moderate but acceptable size distribution. A zeta potential of -40.9 ± 1.17 mV indicates strong electrostatic repulsion and excellent colloidal stability, supporting sustained dispersion of the nanoparticles. Additionally, conductivity testing demonstrated that the apigenin-silver nanoparticle-embedded hydrogel successfully completed a circuit and powered an LED, validating its electrical functionality.

This study successfully fabricated and characterized a conductive nanocomposite suitable for epicardial cardiac patch integration. The synthesized material showed uniform nanostructure, strong colloidal stability, and functional surface chemistry. Its ability to propagate electrical signals within a hydrogel matrix confirms its potential to restore conductivity in infarcted myocardial regions. These findings support its application in next-generation cardiac patches, offering both mechanical support and electrical signal restoration. Future work will involve biological evaluation and integration with mechanically optimized patch architectures.

ACKNOWLEDGEMENT

The authors would like to acknowledge and appreciate the Ministry of Higher Education Malaysia for the Fundamental Research Grant Scheme (FRGS) with reference number: FRGS/1/2020/STG05/UTM/02/17 and University Technologi Malaysia Encouragement Research Grant (UTMER) with reference number: Q.J130000.3851.18J88.

REFERENCES

Abdel-Aty, A. M., Barakat, A. Z., Bassuiny, R. I., & Mohamed, S. A. 2023. Statistical optimization, characterization, antioxidant and antibacterial properties of silver nanoparticle biosynthesized by saw palmetto seed phenolic extract. Scientific Reports, 13(1), 15605. https://doi.org/10.1038/s41598-023-42675-0

Agarwala, S. 2020. Electrically conducting hydrogels for health care: Concept, fabrication methods, and applications. International journal of bioprinting, 6(2). doi: 10.18063/ijb.v6i2.273

Al-Ansari, D. E., Mohamed, N. A., Marei, I., Zekri, A., Kameno, Y., Davies, R. P., ... & Abou-Saleh, H. 2020. Internalization of metal–organic framework nanoparticles in human vascular cells: implications for cardiovascular disease therapy. Nanomaterials, 10(6), 1028. https://doi.org/10.3390/nano10061028

Alexis, F., Pridgen, E., Molnar, L. K., & Farokhzad, O. C. .2008. Factors affecting the clearance and biodistribution of polymeric nanoparticles. Molecular Pharmaceutics, 5(4), 505–515. https://doi.org/10.1021/mp800051m

Alkhalaf M.I., Hussein R.H., Hamza A. 2020. Greensynthesis ofsilver nanoparticles by Nigella sativa extract alleviates diabetic neuropathy through anti-inflammatory and antioxidant effects. Saudi J Biol Sci. 27:2410–9. doi: 10.1016/j.sjbs.2020.05. 005

Cervantes, B., Arana, L., Murillo-Cuesta, S., Bruno, M., Alkorta, I., Varela-Nieto, I. 2019. Solid Lipid Nanoparticles Loaded with Glucocorticoids Protect Auditory Cells from Cisplatin-Induced Ototoxicity. J. Clin. Med. 2019, 8, No. 1464. doi: 10.3390/jcm8091464

Danaei, M., Dehghankhold, M., Ataei, S., Hasanzadeh Davarani, F., Javanmard, R., Dokhani, A., Khorasani, S., & Mozafari, M. R. 2018. Impact of particle size and polydispersity index on the clinical applications of lipidic nanocarrier systems. Pharmaceutics, 10(2), 57. https://doi.org/10.3390/pharmaceutics10020057

Ekren, S., Sönmez, Ç., Sancaktaroğlu, S., & Bayram, E. 2007. Farklı biçim yüksekliklerinin adaçayı (Salvia officinalis L.) genotiplerinde agronomik ve teknolojik özelliklere etkisinin belirlenmesi. Ege Üniversitesi Ziraat Fakültesi Dergisi, 44(1), 55-70.

El-Baz, Y. G., Moustafa, A., Ali, M. A., El-Desoky, G. E., Wabaidur, S. M., & Iqbal, A. 2023. Green synthesized silver nanoparticles for the treatment of diabetes and the related complications of hyperlipidemia and oxidative stress in diabetic rats. Experimental Biology and Medicine, 248(23), 2237-2248. doi: 10.1177/15353702231214258.

Ghiuță, I., & Cristea, D. 2020. Silver nanoparticles for delivery purposes. In Nanoengineered biomaterials for advanced drug delivery (pp. 347-371). Elsevier. doi: 10.1016/B978-0-08-102985-5.00015-2

Haripriyaa, M., & Suthindhiran, K. 2023. Pharmacokinetics of nanoparticles: current knowledge, future directions and its implications in drug delivery. Future Journal of Pharmaceutical Sciences, 9(1), 113. https://doi.org/10.1186/s43094-023-00569-y

Hasan, A., Morshed, M., Memic, A., Hassan, S., Webster, T. J., & Marei, H. E. S. 2018. Nanoparticles in tissue engineering: applications, challenges and prospects. International journal of nanomedicine, 5637-5655. doi: 10.2147/IJN.S153758

Hemlata, Meena, P. R., Singh, A. P., & Tejavath, K. K. 2020. Biosynthesis of silver nanoparticles using Cucumis prophetarum aqueous leaf extract and their antibacterial and antiproliferative activity against cancer cell lines. *ACS omega*, *5*(10), 5520-5528. doi: 10.1021/acsomega.0c00155.

Hinderer, S., & Schenke-Layland, K. 2019. Cardiac fibrosis–a short review of causes and therapeutic strategies. Advanced drug delivery reviews, 146, 77-82. doi: 10.1016/j.addr.2019.05.011.

Hosoyama K. Multi-functional thermo-crosslinkable collagen-metal nanoparticle composites for tissue regeneration: Nanosilver vs. nanogold. 2017. RSC Adv. 7:47704–47708. doi: 10.1039/C7RA08960K.

Li L, Bi Z, Hu Y, Sun L, Song Y, Chen S, et al. Silver nanoparticles and silver ions cause inflammatory response through induction of cell necrosis and the release of mitochondria in vivo and in vitro. Cell Biol Toxicol. (2021) 37:177–91. doi: 10.1007/s10565-020-09526-4.

Liang, J., Guo, Z., Timmerman, A., Grijpma, D., & Poot, A. 2019. Enhanced mechanical and cell adhesive properties of photo-crosslinked PEG hydrogels by incorporation of gelatin in the networks. *Biomedical Materials*, *14*(2), 024102. DOI: 10.1088/1748-605X/aaf31b

Liang, Y., Qiao, L., Qiao, B., & Guo, B. (2023). Conductive hydrogels for tissue repair. Chemical Science, 14(12), 3091-3116.https://doi.org/10.1039/D3SC00145H

Mariadoss, A. V. A., Ramachandran, V., Shalini, V.;, Agilan, B., Franklin, J. H., Sanjay, K., Alaa, Y. G., Tawfiq, M. A.,

© 2025 Penerbit UTM Press. All rights reserved

Ernest, D. 2019. Green synthesis, characterization and antibacterial activity of silver nanoparticles by Malus domestica and its cytotoxic effect on (MCF-7) cell line. Microb. Pathog. 2019, 135, No. 103609. doi: 10.1016/j.micpath.2019.103609.

Mekonnen, B. T., Ragothaman, M., & Palanisamy, T. 2017. Bifunctional hybrid composites from collagen biowastes for heterogeneous applications. ACS omega, 2(8), 5260-5270. doi: 10.1021/acsomega.7b01011

Mohammed, A. E., Bin Baz, F. F., Albrahim, J. S. 2018. Calligonum comosum and Fusarium sp. extracts as bio-mediator in silver nanoparticles formation: characterization, antioxidant and antibacterial capability. 3 Biotech 2018, 8, No. 72. doi: 10.1007/s13205-017-1046-5.

Mukaratirwa-Muchanyereyi, N., Gusha, C., Mujuru, M., Guyo, U., & Nyoni, S. 2022. Synthesis of silver nanoparticles using plant extracts from Erythrina abyssinica aerial parts and assessment of their anti-bacterial and anti-oxidant activities. Results in Chemistry, 4, 100402. https://doi.org/10.1016/j.rechem.2022.100402

Nguyen, H. L., Jo, Y. K., Cha, M., Cha, Y. J., Yoon, D. K., Sanandiya, N. D., ... & Hwang, D. S. 2016. Mussel-inspired anisotropic nanocellulose and silver nanoparticle composite with improved mechanical properties, electrical conductivity and antibacterial activity. Polymers, 8(3), 102. https://doi.org/10.3390/polym8030102

Njud S. Alharbi, Nehad S. Alsubhi, Afnan I. Felimban , Green synthesis of silver nanoparticles using medicinal plants: Characterization and application. 2022. Journal of Radiation Research and Applied Sciences, 5, Issue 3,109-124, https://doi.org/10.1016/j.jrras.2022.06.012.

Olugbodi, J. O., Lawal, B., Bako, G., Onikanni, A. S., Abolenin, S. M., Mohammud, S. S., ... & Batiha, G. E. S. 2023. Effect of sub-dermal exposure of silver nanoparticles on hepatic, renal and cardiac functions accompanying oxidative damage in male Wistar rats. Scientific Reports, 13(1), 10539. doi: 10.1038/s41598-023-37178-x.

Raberi, V. S., Esmati, M., Bodagh, H., Ghasemi, R., Ghazal, M., Matinpour, A., & Abbasnezhad, M. 2022. The Functionality of Apigenin as a Novel Cardioprotective Nutraceutical with Emphasize on Regulating Cardiac Micro RNAs:-. Galen Medical Journal, 11, e2535. doi: 10.31661/gmj.v11i.2535

Sarangi, B., Aggarwal, S. G., & Gupta, P. K. 2017. Performance check of particle size standards within and after shelf-life using differential mobility analyzer. Journal of Aerosol Science, 103, 24-37. DOI: 10.1016/j.jaerosci.2016.10.002

Shakeel Ahmed, Mudasir Ahmad, Babu Lal Swami, Saiqa Ikram. 2016. A review on plants extract mediated synthesis of silver nanoparticles for antimicrobial applications: A green expertise, Journal of Advanced Research. 7 (1), 17-28. https://doi.org/10.1016/j.jare.2015.02.007.

Shao, H., Zhang, T., Gong, Y., & He, Y. 2023. Silver-Containing Biomaterials for Biomedical Hard Tissue Implants. Advanced Healthcare Materials. 12(26), 2300932. https://doi.org/10.1002/adhm.202300932

Sheikh, K., & Shahrajabian, H. 2021. Experimental study on mechanical, thermal and antibacterial properties of hybrid nanocomposites of PLA/CNF/AG. International Journal of Engineering, 34(2),500-507. doi:10.5829/ije.2021.34.02b.23.

Song, X., Wang, X., Zhang, J., Shen, S., Yin, W., Ye, G., ... & Qiu, X. 2021. A tunable self-healing ionic hydrogel with microscopic homogeneous conductivity as a cardiac patch for myocardial infarction repair. Biomaterials, 273, 120811. https://doi.org/ 10.1016/j.biomaterials.2021.120811

Swati Jaast, Anita Grewal, Green synthesis of silver nanoparticles, characterization and evaluation of their photocatalytic dye degradation activity. 2021. Current Research in Green and Sustainable Chemistry. 4,100195. https://doi.org/10.1016/j.crgsc.2021.100195.

Talabani, R. F., Hamad, S. M., Barzinjy, A. A., & Demir, U. 2021. Biosynthesis of silver nanoparticles and their applications in harvesting sunlight for solar thermal generation. Nanomaterials, 11(9), 2421. https://doi.org/10.3390/nano11092421

Talarska, P., Boruczkowski, M., & Żurawski, J. 2021. Current knowledge of silver and gold nanoparticles in laboratory research—application, toxicity, cellular uptake. Nanomaterials. 1(9), 2454. https://doi.org/10.3390/nano11092454

Thomas, S. D., Jha, N. K., Jha, S. K., Sadek, B., & Ojha, S. 2023. Pharmacological and molecular insight on the cardioprotective role of apigenin. Nutrients, 15(2), 385. doi: 10.3390/nu15020385

Tsao, C.W., Aday, A.W., Almarzooq, Z.I., Alonso, A., Beaton, A.Z., Bittencourt, M.S., Boehme, A.K., Buxton, A.E., Carson, A.P., Commodore-Mensah, Y. and Elkind, M.S., 2022. Heart disease and stroke statistics—2022 update: a report from the American Heart Association. *Circulation*, *145*(8),e153-e639. https://doi.org/10.1161/CIR.0000000000001052.

Wan Mat Khalir, W. K. A., Shameli, K., Jazayeri, S. D., Othman, N. A., Che Jusoh, N. W., & Hassan, N. M. 2020. Biosynthesized silver nanoparticles by aqueous stem extract of Entada spiralis and screening of their biomedical activity. Frontiers in chemistry, 8, 620. doi: 10.3389/fchem.2020.00620.

Wei, X., Wang, L., Duan, C., Chen, K., Li, X., Guo, X., ... & Fan, Y. 2023. Cardiac patches made of brown adipose-derived stem cell sheets and conductive electrospun nanofibers restore infarcted heart for ischemic myocardial infarction. Bioactive Materials' 27, 271-287. https://doi.org/10.1016/j.bioactmat.2023.03.023

Xu, L., Wang, Y. Y., Huang, J., Chen, C. Y., Wang, Z. X., & Xie, H. 2020. Silver nanoparticles: Synthesis, medical applications and biosafety. Theranostics, 10(20), 8996. doi: 10.7150/thno.45413

Younis, N. K., Ghoubaira, J. A., Bassil, E. P., Tantawi, H. N., & Eid, A. H. 2021. Metal-based nanoparticles: Promising tools for the management of cardiovascular diseases. Nanomedicine: Nanotechnology, Biology and Medicine, 36, 102433. doi: 10.1016/j.nano.2021.102433.

Zheng, Z., Tan, Y., Li, Y., Liu, Y., Yi, G., Yu, C.Y. and Wei, H., 2021. Biotherapeutic-loaded injectable hydrogels as a synergistic strategy to support myocardial repair after myocardial infarction. Journal of Controlled Release, 335, 216-236. https://doi.org/ 10.1016/j.jconrel.2021.05.023

© 2025 Penerbit UTM Press. All rights reserved